Seidel Aberrations of a Slightly Decentred Optical System

Janina Bartkowska, Zygmunt Bartkowski***

The "second" order aberrations in Seidel's space are described for a system composed of slightly decentred spherical or plane surfaces, assuming the system without any symmetry. Six vector coefficients of the aberrations appear here. These vectors are formed by a linear superposition of the decentration vectors with certain scalar aberration coefficients.

The scalar aberration coefficients of several surfaces can be easily computed, if the 3-rd order aberrations of the centered system are known.

Introduction

Many authors investigated the properties of the slightly decentred systems. Maréchal [5] examined the wave aberrations of systems without either symmetry axis or symmetry plane, composed of two parts with skew optical axis. In his paper the aberrations of decentration are related to wave aberrations in an indirect space. He describes coma, astigmatism and the inclination of the image and the distortion. The third and higher order aberrations of decentration have been described by Cox [3]. He has asserted that two inclined planes are the astigmatic image of a plane perpendicular to axis. In his book the parameters of decentration of a surface are the coordinates of its center with respect to the axis of reference. In Hoffman's papers [4] the main subject was a rational definition of decentrations.

But all these works do not specify clearly, how the influences of decentration of several surfaces can be summed in the case of a system without either axis or plane of symmetry. The assertion that the astigmatic image of a plane forms two planes does not seem right to us.

The purpose of this work consists in the examination of the images of points, lines and planes. Especially important for us was the examination of the laws, after which the influences of decentration of several surfaces sum up for the final aberrations. Our own experience shows that the 2-nd order aberrations give satisfactory results for the systems with large apertures too. Therefore the power series expansion method with omission of higher order terms has been applied. It is assumed that the axis of reference of the decentred system passes through the center of diaphragm and is perpendicular to the object and diaphragm plane. The centers of the curvature of the several spherical refracting surfaces lie at small distances from the axis of reference, and the normals to refracting planes make small angles with the axis. The optical system to be examined does not possess either symmetry axis or symmetry plane. The distances of the centres of curvature from the axis of reference are small vectors perpendicular to this axis, and some of them can be skew ones with respect to others. In general the centres of curvature of several surfaces of the system will not be in the same plane.

* J. Bartkowska, Centralne Laboratorium Optyki, Warszawa ul. Kamionkowska 18, Poland.

** Z. Bartkowski, PIHM, Warszawa, ul. Podleśna 61, Poland.

Decentred surface

The ordinary equation of the centered sphere, with respect to an origin at the vertex is [3]

$$(x^2+y^2+z^2)\varrho-2x = 0, \tag{1}$$

$\varrho = \frac{1}{R}$ where R is the radius of the sphere.

Now, let us consider a light ray from the object point $A(s, L_y, L_z)$ incident on the plane of entrance pupil at the point $B(p, M_y, M_z)$. If the directional cosines of the incident ray are α, β and γ the equations of the ray may be written as

$$y = L_y+\frac{\beta}{\alpha}(x-s) \tag{2}$$

or

$$y = \frac{L_y p-M_y s}{p-s}+\frac{x(M_y-L_y)}{p-s}; \tag{3}$$

x, y, z denote the coordinates of any point lying on the ray. Analogous equations may be written for the z-coordinates. In what follows the relationships for the z-coordinates will be omitted since they can be easily reproduced replacing y by z and β by γ. We also assume the vectors $\boldsymbol{M}(0, M_y, M_z)$ and $\boldsymbol{L}(0, L_y, L_z)$ small enough to neglect the terms of order higher than third. The directional cosines of the incident ray are to the first approximation:

$$\alpha = 1-\frac{(\boldsymbol{M}-\boldsymbol{L})^2}{2(p-s)^2}+\ldots$$

$$\beta = \frac{M_y-L_y}{p-s}\alpha. \tag{4}$$

Substituting formulas (2) for y and z in Eq. (1) we obtain the coordinates of the point of incidence on the spherical surface. We take into account a point $D(x, y, z)$ near to the coordinate origin (3)

$$x = \frac{(\boldsymbol{M}s-\boldsymbol{L}p)^2}{2(p-s)^2}\varrho+\ldots$$

$$y = \frac{L_y p-M_y s}{p-s}+\frac{M_y-L_y}{2(p-s)^3}(\boldsymbol{M}s-\boldsymbol{L}p)^2\varrho+\ldots \tag{5}$$

Differentiating now the equation (1) we find the components of the unit vector normal to the surface at the incidence point

$$\begin{aligned} N_x &= 1-x\varrho, \\ N_y &= -y\varrho, \\ N_z &= -z\varrho. \end{aligned} \tag{6}$$

The direction of the normal is chosen to form an acute angle with the incident ray. The cosine of the angle of incidence is determined by the scalar product of the vectors of the normal and of the incident ray

$$\cos i = \alpha-\varrho(x\alpha+y\beta+z\gamma). \tag{7}$$

Applying the law of refraction we obtain for the cosine of the refraction angle i'

$$\cos i' = \sqrt{1-\frac{n^2}{n'^2}+\frac{n^2}{n'^2}\cos^2 i}. \tag{8}$$

The replacing of x, y, z, α, β and γ in (7) by their approximate values from (4) and (5) allows us to write in this approximation

$$\cos i = 1 - \frac{1}{2(p-s)^2}[\boldsymbol{M}(1-\varrho s) - \boldsymbol{L}(1-\varrho p)]^2. \tag{9}$$

Substituting this expression to (8), expanding the corresponding square root into a power series

$$\sqrt{1-t} = 1 - \frac{t}{2} - \frac{t^2}{8} + \ldots \tag{10}$$

and omitting the terms of order higher than two we have

$$\cos i' = 1 - \frac{n^2}{2n'^2(p-s)^2}[\boldsymbol{M}(1-\varrho s) - \boldsymbol{L}(1-\varrho p)]^2.$$

Let the considered spherical surface be displaced by a small vector $\boldsymbol{c}$ perpendicular to the axis of reference. Its equation is the following (3)

$$[x^2 + (y-c_y)^2 + (z-c_z)^2]\varrho - 2x = 0. \tag{11}$$

This displacement is small enough to neglect the terms quadratic in $\boldsymbol{c}$. The incident ray meets the decentred surface at the point D^* with the coordinates

$$\begin{aligned} x^* &= x + \delta x, \\ y^* &= y + \delta y. \end{aligned} \tag{12}$$

From Eq. (2) it follows that

$$\delta y = \frac{\beta}{\alpha}\delta x. \tag{13}$$

From the relationships (11), (12) and (13), omitting terms of higher order, we obtain

$$\begin{aligned} \delta x &= \frac{\boldsymbol{c}}{p-s}\cdot(\boldsymbol{M}s - \boldsymbol{L}p), \\ \delta y &= \frac{\boldsymbol{c}}{(p-s)^2}\cdot(\boldsymbol{M}s - \boldsymbol{L}p)(M_y - L_y). \end{aligned} \tag{14}$$

In the formulas (14) the scalar products

$$\begin{aligned} \boldsymbol{c}\cdot\boldsymbol{M} &= c_y M_y + c_z M_z, \\ \boldsymbol{c}\cdot\boldsymbol{L} &= c_y L_y + c_z L_z \end{aligned} \tag{15}$$

appear.

Differentiating Eq. (11) we find the components of the vector normal to the decentred surface at the point of incidence

$$\begin{aligned} N_x^* &= N_x - \varrho\delta x, \\ N_y^* &= N_y + \varrho c_y - \varrho\delta y, \end{aligned} \tag{16}$$

where N_x and N_y are given by the formulas (6). Now, using (1) and the approximate expressions (4), (5), (15) and (16) we obtain for the angles of incidence and refraction

$$\begin{aligned} \cos^* i &= \cos i + \frac{\varrho\boldsymbol{c}}{p-s}[\boldsymbol{M}(1-\varrho s) - \boldsymbol{L}(1-\varrho p)], \\ \cos^* i' &= \cos i' + \frac{n^2}{n'^2}\frac{\varrho\boldsymbol{c}}{(p-s)}[\boldsymbol{M}(1-\varrho s) - \boldsymbol{L}(1-\varrho p)]. \end{aligned} \tag{17}$$

The directional cosines of the refracted ray on any surface are given by the formulas (3)

$$\begin{aligned} n'\alpha' &= n\alpha+N_x(n'\cos i'-n\cos i), \\ n'\beta' &= n\beta+N_y(n'\cos i'-n\cos i). \end{aligned} \tag{18}$$

With the help of (4), (5), (6), (9) and (18) and the law of refraction

$$\frac{n'}{s'} = \frac{n}{s}+(n'-n)\varrho, \tag{19}$$

(s' — Gaussian image distance) we obtain the following approximate expressions

$$\alpha' = 1-\frac{1}{2(p-s)^2}\left(\frac{Ms}{s'}-\frac{Lp}{p'}\right)^2,$$

$$\begin{aligned} \beta' = {} & \frac{1}{p-s}\left(\frac{M_y s}{s'}-\frac{L_y p}{p'}\right)+\frac{\Delta n\varrho}{2n'(p-s)^3}\Bigg\{M_y M^2\left[\frac{sn}{n'}(1-\varrho s)^2-\varrho s^2\right]+ \\ & +2M_y ML\left[-\frac{sn}{n'}(1-\varrho s)(1-\varrho p)+\varrho sp\right]+M^2L_y\left[-\frac{pn}{n'}(1-\varrho s)^2+\varrho s^2\right]+ \\ & +M_y L^2\left[\frac{sn}{n'}(1-\varrho p)^2-\varrho p^2\right]+2MLL_y\left[\frac{pn}{n'}(1-\varrho s)(1-\varrho p)-\varrho sp\right]+ \\ & +L_y L^2\left[-\frac{np}{n'}(1-\varrho p)^2+\varrho p^2\right]\Bigg\}+\frac{n}{2(p-s)^3n'}(M-L)^2(L_y-M_y). \end{aligned} \tag{20}$$

The equation of the refracted ray is

$$Y = y+\frac{\beta'}{\alpha'}(X-x). \tag{21}$$

The coordinates of the intersection point of the refraction ray with the Gaussian image plane are determined by the equation

$$L'_y = y+\frac{\beta'}{\alpha'}(s'-x). \tag{21a}$$

Since α' appears in the denominator we use the following expansion

$$\frac{1}{\alpha'} = \frac{1}{1-t} = 1+t+t^2+\ldots \tag{22}$$

It is convenient to introduce angular coordinates for both the paraxial aperture rays and the paraxial principal rays

$$\begin{aligned} \sigma &= \frac{h}{s};\ \omega = \frac{y}{p}, \\ i &= \sigma-h\varrho;\ j = \omega-y\varrho. \end{aligned} \tag{23}$$

where h and y denote the "paraxial" height of rays, σ and ω angles with respect to the coordinate axis, i and j angles of incidence.

Using the symbols (23) and approximations (5), (19) the formula (21a) becomes

$$\begin{aligned} L'_y = {} & \frac{L_y n\sigma}{n'\sigma'}+\frac{1}{2(p-s)^3\sigma'n'}\Bigg[M_y M^2\frac{S_{\mathrm{I}}}{\sigma^3}-\frac{(M^2L_y+2M_yML)}{\sigma^2\omega}S_{\mathrm{II}}+ \\ & +\frac{M_yL^2}{\sigma\omega^2}(S_{\mathrm{III}}+J^2S_{\mathrm{IV}})+\frac{2MLL_y}{\sigma\omega^2}S_{\mathrm{III}}-\frac{L_yL^2}{\omega^3}S_{\mathrm{V}}\Bigg]. \end{aligned} \tag{24}$$

We denote

$$S_{\rm I} = hn^2 i^2 \Delta \frac{\sigma}{n}, \quad S_{\rm II} = hn^2 ij \Delta \frac{\sigma}{n},$$

$$S_{\rm III} = hn^2 j^2 \Delta \frac{\sigma}{n}, \quad S_{\rm IV} = -\varrho \Delta \frac{1}{n}, \tag{25}$$

$$S_{\rm V} = hn^2 n^2 \Delta \frac{\omega}{n} + JynjS_{\rm IV}, \quad J = n(y\sigma - h\omega).$$

The formula (24) represents the generalization of the known expressions for the transverse aberrations of the third order. Writing now analogous formula for the z-coordinate, expanding scalar products and substituting $L_z = 0$, we obtain known formulas for the third order aberrations.

Similar calculations may be repeated for the ray refracted at the decentred surface. From the formula (17) and (12) to (16), it follows

$$\alpha'^* = \alpha' + \frac{\Delta n \varrho \boldsymbol{c}}{n'(p-s)} \cdot \left(\frac{\boldsymbol{L}p}{p'} - \frac{\boldsymbol{M}s}{s'}\right), \tag{26}$$

$$\beta'^* = \beta' + \frac{\varrho c_y \Delta n}{n'} + \frac{\varrho c_y n \Delta n'}{2n'^2(p-s)^2} [\boldsymbol{M}(1-\varrho s) - \boldsymbol{L}(1-\varrho p)]^2 +$$
$$+ \frac{\Delta n \varrho^2 \boldsymbol{c}}{n'(p-s)^2} \cdot \left\{(\boldsymbol{L}p - \boldsymbol{M}s)(M_y - L_y) + \frac{n}{n'}(L_y p - M_y s)[\boldsymbol{M}(1 \varrho s) - \boldsymbol{L}(1-\varrho p)]^2\right\}.$$

The formula (21) determines now the coordinates of the intersection point with the Gaussian image plane. We can rewrite it as follows

$$L'_y = y + \delta y + \frac{\beta'^*}{\alpha'^*}(s' - x - \delta x). \tag{27}$$

Now, substituting x, δx, y, δy, α'^*, β'^* and γ'^* in (27) by their approximations from (4), (5) (9), (14), (20), (26) and using (19), (23) and the expansion (22), we obtain

$$L'^*_y = L'_y + \frac{\varrho c_y \Delta(ns')}{n'} + \frac{ss'n^2\varrho}{n'(p-s)^2}\left[(\varrho s - 1)\Delta\left(\frac{1}{ns}\right)\left(\frac{c_y \boldsymbol{M}^2}{2} + \boldsymbol{c}\boldsymbol{M}M_y\right) + \right.$$
$$\left. + (1-\varrho p)\Delta\left(\frac{1}{ns}\right)(c_y \boldsymbol{M}\boldsymbol{L} + L_y \boldsymbol{c}\boldsymbol{M} + M_y \boldsymbol{c}\boldsymbol{L}) + \frac{(s-p)\Delta n}{s^2 nn'} M_y \boldsymbol{c}\boldsymbol{L}\right] +$$
$$+ \frac{\varrho s' pn^2}{n'(p-s)^2}\left\{\frac{c_y \boldsymbol{L}^2}{2}\left[(\varrho p - 1)\Delta\left(\frac{1}{np}\right) + \frac{\varrho \Delta n}{nn's}(s-p)\right] + \right.$$
$$\left. + L_y \boldsymbol{c}\boldsymbol{L}\left[(\varrho p - 1)\Delta\left(\frac{1}{np}\right) + \frac{(\varrho p - 1)\Delta n(s-p)}{nn'ps}\right]\right\}. \tag{28}$$

The coordinates of the point of intersection of the ray refracted at the decentred surface with the Gaussian image plane of diaphragm can be calculated in the same manner

$$M'^*_y = M'_y + \frac{\varrho c_y \Delta np'}{n'} + \dots$$
$$M'_y = M_y \frac{n\omega}{n'\omega'} + \dots \tag{29}$$

Aberrations of a system of decentred surfaces

Repeating above considerations step by step for each surface of the decentred system we obtain the aberrations in the space of the final image. The image produced by the first surface is treated as the object for the second and so on. We omit the products of vectors $\boldsymbol{c}$. The formulas (26) and

(28) are valid, if the diaphragm is situated before the decentred surfaces of the system. If the diaphragm is inside then its image is formed by the antecedent decentred part of the system. As it is evident from (29) its displacement may be written as follows:

$$M_y^* = M_y - \frac{1}{n\omega} \sum_{1}^{l} c_y \varrho y \Delta n + \ldots \tag{30}$$

The summation extends over all the decentred surfaces between the object and the diaphragm. Substituting $\boldsymbol{M}^*$ for $\boldsymbol{M}$ in the formula (24) for the surfaces lying between object and the diaphragm we obtain additional aberration term due to the decentring of the entrance pupil.

The final formula for the coordinates of the point of intersection of the refracted ray with the plane of the Gaussian image may be written in the following way

$$\begin{aligned} L_y'^* = {} & L_y' + \frac{1}{\sigma' n'} \Sigma C_{\mathrm{I},k} \varrho_k c_{k,y} + \frac{n^2}{b' \sigma' J^2} \Bigg\{ \Bigg[\left(\frac{\boldsymbol{M}^2}{2} + M_y^2 \right) \Sigma c_{k,y} \varrho_k C_{\mathrm{II},k} + \\ & + M_z M_y \Sigma c_{k,z} \varrho_k C_{\mathrm{II},k} \Bigg] \omega^2 - \sigma\omega [(3 M_y L_y + M_z L_z) \Sigma c_{k,y} \varrho_k C_{\mathrm{III},k} + \\ & + (M_z L_y + M_y L_z) \Sigma c_{k,z} \varrho_k C_{\mathrm{III},k} + J^2 M_y (L_y \Sigma \varrho_k c_{k,y} C_{\mathrm{IV},k} + L_z \Sigma \varrho_k c_{k,z} C_{\mathrm{IV}})] + \\ & + \sigma \left[\left(\frac{\boldsymbol{L}^2}{2} + L_y^2 \right) \Sigma c_{k,y} \varrho_k C_{\mathrm{V},k} + L_y L_z \Sigma c_{k,z} \varrho_k C_{\mathrm{V},k} + \frac{\boldsymbol{L}^2 J^2}{2} \Sigma \varrho_k c_{k,y}' C_{\mathrm{VI},k} \right] \Bigg\}. \end{aligned} \tag{31}$$

Interchanging the indices y and z we obtain the formula for the coordinate L_z'. The summation is extending over all the decentred surfaces. The formula (31) contains 6 independent aberration coefficients. They differ in the case of the surfaces lying before or after the diaphragm. To make them uniform, what is convenient for the calculations on computers, we introduce an auxiliary symbol

$\theta = 0$ for the surfaces lying after the diaphragm,

$\theta = -1$ for the surfaces lying before the diaphragm.

The coefficients C can be computed easily, if the third order aberrations are known (25) and angular coordinates of both the auxiliary rays (23) for the corresponding centred system.

$$\begin{aligned} C_{\mathrm{I},k} &= h_k \Delta_k n, \\ C_{\mathrm{II},k} &= -n_k^2 h_k i_k \Delta_k \left(\frac{\sigma}{n} \right) + \frac{\Delta_k n}{J} \left[y_k \Big(\sum_{k+1}^{p} S_{\mathrm{I}} + \theta \sum_{1}^{p} S_{\mathrm{I}} \Big) - h_k \sum_{k+1}^{p} S_{\mathrm{II}} \right], \\ C_{\mathrm{III},k} &= -n_k^2 h_k j_k \Delta_k \left(\frac{\sigma}{n} \right) + \frac{\Delta_k n}{J} \left[y_k \Big(\sum_{k+1}^{p} S_{\mathrm{II}} + \theta \sum_{1}^{p} S_{\mathrm{II}} \Big) - h_k \sum_{k+1}^{p} S_{\mathrm{III}} \right], \\ C_{\mathrm{IV},k} &= -\frac{\sigma_k n_k}{J} \Delta_k \left(\frac{1}{n} \right) - \frac{\Delta_k n}{J} h_k \sum_{k+1}^{p} S_{\mathrm{IV}}, \\ C_{\mathrm{V},k} &= -n_k^2 j_k h_k \Delta_k \left(\frac{\omega}{n} \right) - n_k j_k J \Delta_k \left(\frac{1}{n} \right) + \frac{\Delta_k n}{J} \left[y_k \Big(\sum_{k+1}^{p} S_{\mathrm{III}} + \theta \sum_{1}^{p} S_{\mathrm{III}} \Big) - h_k \sum_{k+1}^{p} S_{\mathrm{V}} \right], \\ C_{\mathrm{VI}} &= \frac{\omega_k}{n_k J} \Delta_k \left(\frac{1}{n} \right) + \frac{\Delta_k n}{J} y_k \Big(\sum_{k+1}^{p} S_{\mathrm{IV}} + \theta \sum_{1}^{p} S_{\mathrm{IV}} \Big). \end{aligned} \tag{32}$$

The summation is extended over all centred or decentred surfaces lying after the considered surface, or over all surfaces of the system. Only C_{I} and C_{IV} do not depend on the position of the diaphragm.

We define the decentration aberrations as the differences between the aberrations of the decentred system and of the corresponding centred system. In other words the decentration aberrations characterise the influence of the decentration on the image quality. It may be easily seen that the formulas (28) and (31) represent the aberrations of the second order. Only the first term does not depend either on the aperture or on the field angle. The second term is proportional to the square of the aperture. The two subsequent aberrations are proportional to the product of the aperture and field magnitude. The last terms are proportional to the square of the field magnitude.

Now, we take into consideration each aberration term separately. Both aberration coordinates may be regarded as the components of a certain vector, whose magnitude and direction depend on the vectors of the surface decentration and on the aberration coefficients.

Beating of the image. Coma

As the first step we examine the first term independent either of the aperture or of the field angle. One may define a resultant vector to be the resultant of the vectors $\boldsymbol{c}$, determining the decentrations of the several surfaces by their curvatures and coefficients C_{I}

$$\boldsymbol{K}_{\mathrm{I}} = \sum_{k=1}^{\nu} \varrho_k \boldsymbol{c}_k C_{\mathrm{I},k}.$$

The vector $\boldsymbol{K}_{\mathrm{I}}$ perpendicular to the axis of reference determines the magnitude and direction of the image beating.

$$\delta \boldsymbol{L}_{\mathrm{I}}' = \frac{1}{n'\sigma'} \boldsymbol{K}_{\mathrm{I}}.$$

This effect causes many unprofitable phenomena, such as the errors of the axis in geodetic instruments and so on. This effect was considered in our previous papers [1], [2].

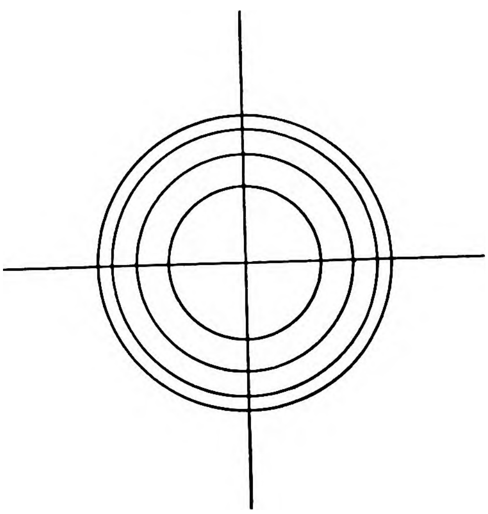

Fig. 1. Rays at entrance pupil

In the same manner we define a resultant vector to be the superposition of the vectors of decentration of several surfaces of the system multiplied by their curvatures and coefficients C_{II}. For convenience a constant multiplier is introduced

$$\boldsymbol{K}_{\mathrm{II}} = \frac{n^2 \omega^2}{J^2 n' \sigma'} \sum \boldsymbol{c}_k C_{\mathrm{II},k}. \tag{33}$$

The angle between vector $\boldsymbol{K}_{\mathrm{II}}$ and the axis y is ϑ_2. The angle of the vector $\boldsymbol{M}$ with the axis y is φ and its components are determined by the formulas

$$M_y = M\cos\varphi,$$
$$M_z = M\sin\varphi, \tag{34}$$

where M denotes the magnitude of the vector $\boldsymbol{M}$.

Combining (33) and (34) with (31), we obtain

$$\begin{aligned} \delta L'_{\mathrm{II},y} &= M^2\left[K_{\mathrm{II},y}\left(1+\frac{\cos 2\varphi}{2}\right)+K_{\mathrm{II},z}\frac{\sin 2\varphi}{2}\right], \\ \delta L'_{\mathrm{II},z} &= M^2\left[K_{\mathrm{II},z}\left(1-\cos\frac{2\varphi}{2}\right)+K_{\mathrm{II},y}\frac{\sin 2\varphi}{2}\right]. \end{aligned} \tag{35}$$

A beam of rays, which meets the plane of diaphragm, forming a circle of the radius M, in the plane of the Gaussian image produces a circle described by the equation

$$(Y-K_{\mathrm{II},y}M^2)^2+(Z-K_{\mathrm{II},z}M^2)^2 = \frac{K_{\mathrm{II}}^2 M^4}{4}. \tag{36}$$

The Equation (36) is obtained from the formulas (35) by elimination of the angle 2φ. As it is seen from the Eq. (36) the center of the circle is determined by the end of the vector $M^2\boldsymbol{K}_{\mathrm{II}}$, and its radius is equal to the half of magnitude of this vector. Let the incident rays form in the plane

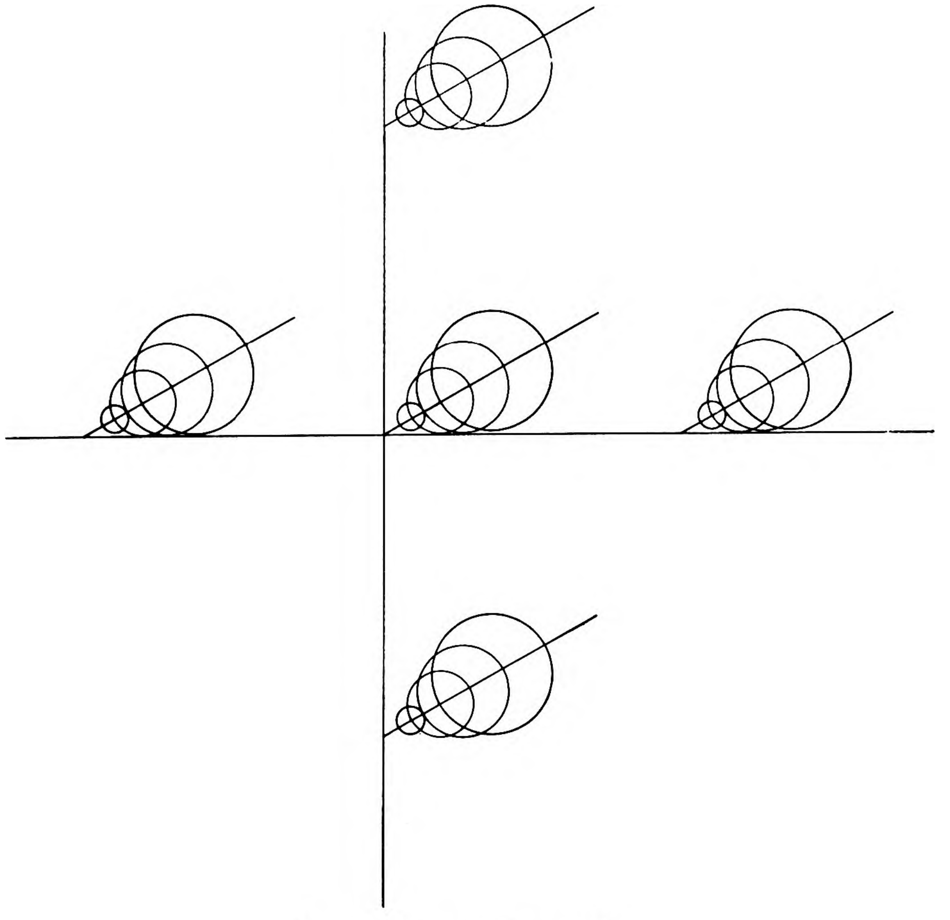

Fig. 2. Coma of decentration

of the diaphragm a family of the concentric rays, as it is shown in the Fig. 1. The squares of the radii of these circles form an arithmetic progression. The aberration images shown in the Fig. 2, form a family of circles, whose centers lie on a straight line, under the angle ϑ_2 to the y-axis, according to the direction of the vector $\boldsymbol{K}_{\mathrm{II}}$. The tangents to these circles cut the y-axis under the angle $\vartheta_2 \pm 30°$. It is clearly a coma. Since this aberration does not depend upon the field of view, the aberration images are identical over the whole field of view [3], [5].

Inclination and astigmatism of the imge

Now, let us consider the aberrations proportional to the product of the magnitude of the field and of the aperture. Two resultant vectors are defined, one as the resultant of the vectors of decentration of the several surfaces multiplied by the coefficients C_{III}, and the second as the resultant of these vectors multiplied by the coefficients C_{IV} and of the doubled vector $\boldsymbol{K}_{III}$, according to the formulas

$$\begin{aligned} \boldsymbol{K}_{III} &= \frac{n^2\sigma\omega}{n'\sigma' J^2}\Sigma \boldsymbol{c}_K \varrho_k C_{III,k}, \\ \boldsymbol{K}_{IV} &= \frac{n^2\sigma\omega}{n'\sigma'}\Sigma \boldsymbol{c}_k \varrho_k C_{IV,k}+2\boldsymbol{K}_{III}. \end{aligned} \tag{37}$$

The angles of both vectors with respect to the y-axis are denoted and by ϑ_3 and ϑ_4, while the angle of vector $\boldsymbol{L}$ with the same axis by ψ. Therefrom it follows that

$$\begin{aligned} L_y &= L\cos\psi, \\ L_z &= L\sin\psi. \end{aligned} \tag{38}$$

Combining (31) with (34), (37) and (38), we obtain

$$\begin{aligned} \delta L'_{III,IV,y} &= -ML[K_{III}\cos(\varphi-\psi-\vartheta_3)+K_{IV}\cos\varphi\cos(\psi-\vartheta_4)], \\ \delta L'_{III,IV,z} &= -ML[K_{III}\sin(\vartheta_3+\psi-\varphi)+K_{IV}\sin\varphi\cos(\psi-\vartheta_4)]. \end{aligned} \tag{39}$$

The formula (39) proves that the rays coming from a circular locus in the plane of the diaphragm intersect the image plane in an ellipse. Squaring both sides of the formulas (39) and adding we obtain the ellipse equation in polar coordinates ϱ and φ

$$\varrho^2 = M^2L^2\left\{[K_{III}+K_{IV}\cos(\psi-\vartheta_4)]^2-4K_{III}K_{IV}\cos(\psi-\vartheta_4)\sin^2\left(\frac{\vartheta_3+\psi}{2}-\varphi\right)\right\}. \tag{40}$$

Its parameters are: the semi-axes

$$\varrho_{1,2} = [K_{IV}\cos(\psi-\vartheta_4)\pm K_{III}]ML. \tag{41}$$

Their angles with the y-axis

$$\varphi_1 = \frac{\vartheta_3+\psi}{2}; \; \varphi_2 = \frac{\vartheta_3+\psi}{2}+90^\circ. \tag{42}$$

The eccentricity

$$e = \frac{2\sqrt{K_{III}K_{IV}\cos(\psi-\vartheta_4)}}{\varrho_1}. \tag{43}$$

The last relationship (43) shows that the ellipses transform into circles in three cases: if $\boldsymbol{K}_{IV} = 0$, $\boldsymbol{K}_{III} = 0$ and, if $\boldsymbol{L}$ is perpendicular to $\boldsymbol{K}_{IV}$.

The Figure 3 corresponds to the case $\boldsymbol{K}_{IV} = 0$. After the formula (41) the circles are observed over the whole field of view. Their radii are proportional to the magnitude of the field, and, what is not visible in the figure, to the magnitude of the diaphragm. The Figure 4 corresponds to the case $\boldsymbol{K}_{III} = 0$, for $\vartheta_4 = 45°$. After the same formula the aberrated images of the points are circles, whose radii depend on the angle between the vectors $\boldsymbol{L}$ and $\boldsymbol{K}_{IV}$. The aberrations dissapear if $\boldsymbol{L}$ is perpendicular to $\boldsymbol{K}_{IV}$. In this case the images of points lying on a straight line passing through the origin and perpendicular to $\boldsymbol{K}_{IV}$ are points. The greatest aberrations arise for the points lying on a line in the direction of the vector $\boldsymbol{K}_{IV}$.

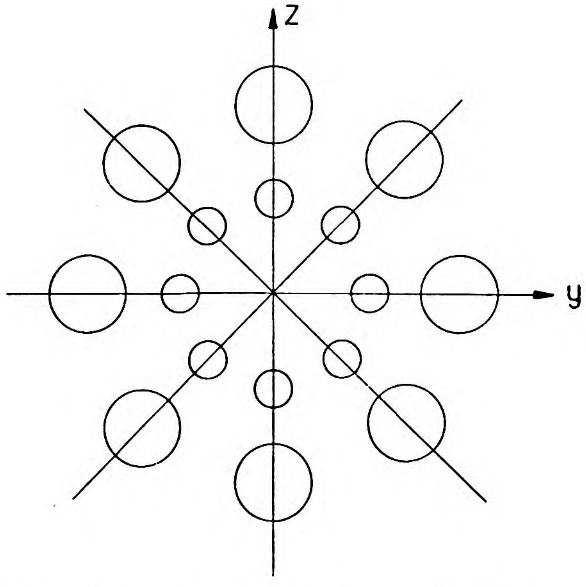

Fig. 3. Astigmatism of decentration if $K_{IV} = 0$

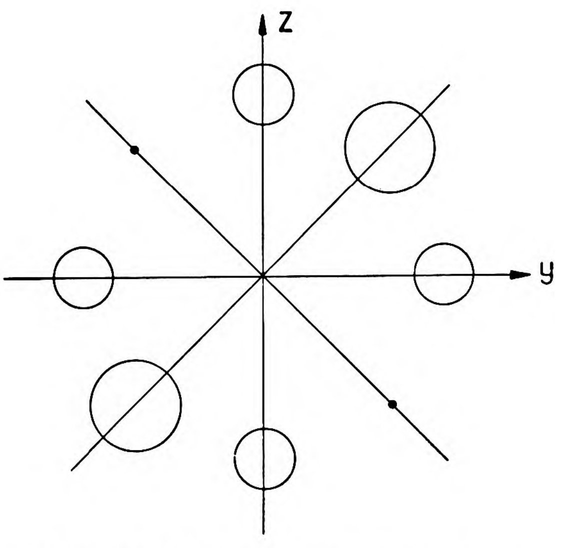

Fig. 4. Inclination of the image if $K_{III} = 0$

The aberrations in the Fig. 5 form circles, ellipses and lines. Both vectors K_{III} and K_{IV} differ from zero and make among themselves the angle 45°, $\vartheta_3 = 0$ and $\vartheta_4 = 45°$. The aberrations curves for the points lying on straight lines directed as the vector K_{IV} form straight lines and, according to (41) and (42), if the line is perpendicular to K_{IV} they are circles. The directions of the symmetry axes of the ellipses are determined by the formulas (42).

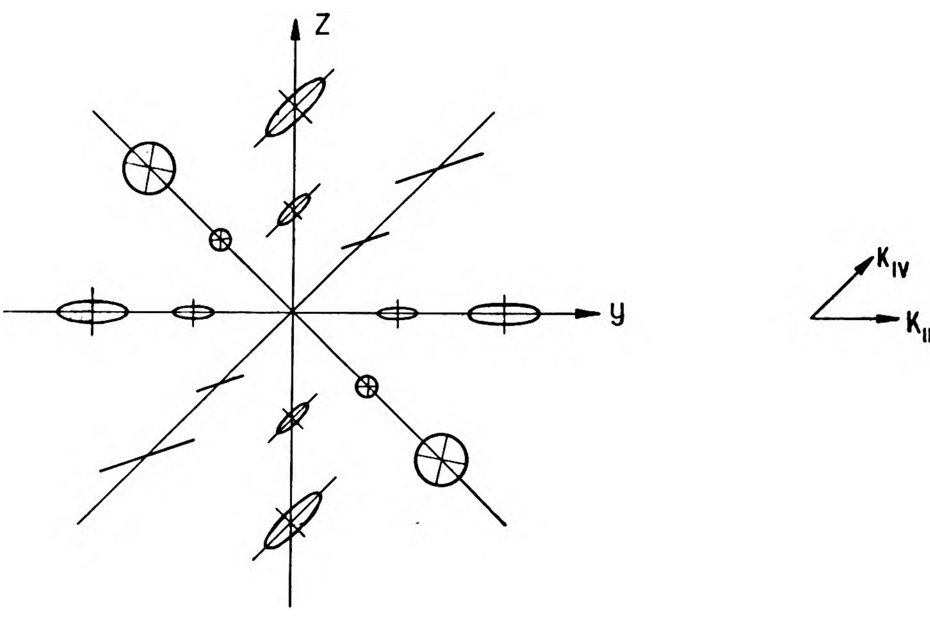

Fig. 5. Astigmatism and image inclination, in general case

In the Fig. 6 both vectors K_{III} and K_{IV} are directed conformably, $\vartheta_3 = \vartheta_4 = 0$. At the same time this common direction plays the role of the axis of symmetry of the figure.

The shape of the aberrations (ellipses and lines) proves the image bundle to be astigmatic. It may be demonstrated, that only those rays intersect with the principal ray, which cut the plane of diaphragm along the lines under the angles φ_1 or φ_2 (42) to the y-axis. All the other rays, which derive from the same object point are skew with respect to the principal ray.

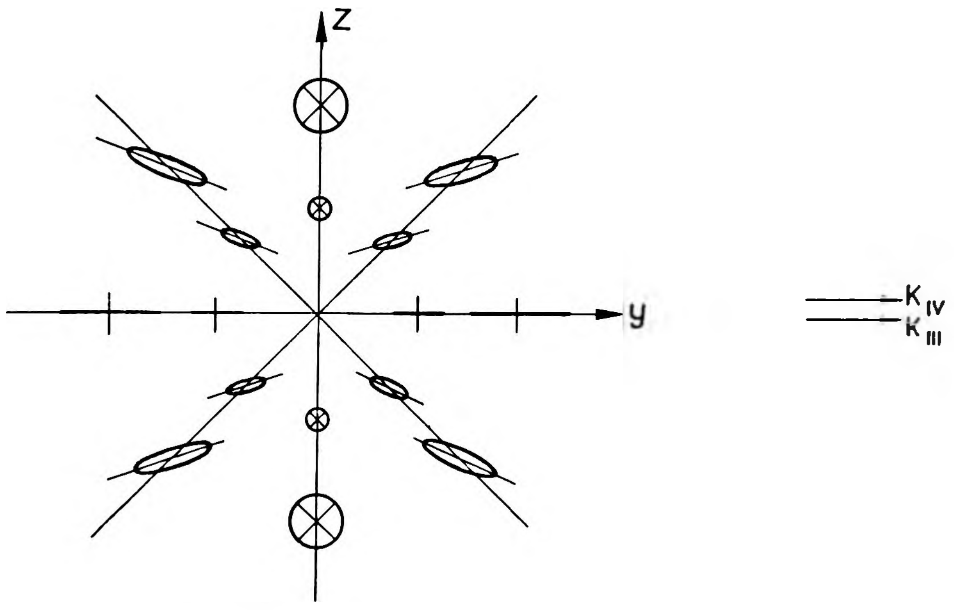

Fig. 6. Astigmatism and image inclination if K_{III} and K_{IV} have the same direction towards themselves and y-axis

According to (2) and (23), (24) the equations of the refracted ray are

$$Y = \frac{L_y n\sigma}{n'\sigma'} + \delta L'_y + \left(\frac{M_y\sigma'}{\sigma} - \frac{L_y\omega'}{\omega}\right)\frac{X}{p-s}. \tag{44}$$

The equation of the principal ray my be obtained assuming in (44) $\boldsymbol{M} = 0$. The ray determined by the Eq. (44) cuts the principal ray if

$$X = -\frac{\delta L'_y(p-s)\sigma}{M_y\sigma'} = -\frac{\delta L'_z(p-s)\sigma}{M_z\sigma'}. \tag{45}$$

It is easy to verify with the help of (39) and (42) that for $\varphi = \varphi_1$

$$\begin{aligned} L'_y &= -ML[K_{III}+K_{IV}\cos(\psi-\vartheta_4)]\cos\frac{\vartheta_3+\psi}{2}, \\ L'_z &= -ML[K_{III}+K_{IV}\cos(\psi-\vartheta_4)]\sin\frac{\vartheta_3+\psi}{2}. \end{aligned} \tag{46}$$

The distance of the point of convergence of the plane bundle of rays from the Gaussian image is the measure of the longitudinal aberration. Applying the same reasoning for $\varphi = \varphi_2$ from (40), (45) and (46) we obtain

$$X = L'_x = L[K_{IV}\cos(\psi-\vartheta_4)\pm K_{III}]\frac{(p-s)\sigma}{\sigma'} \tag{47}$$

for both points of convergence of the astigmatic bundle.

The coordinate Y of the convergence point of the bundle is calculated from (44) assuming $\boldsymbol{M} = 0$ and omitting the terms with the L^2. In the same manner we obtain the Z coordinate. Approximately

$$\begin{aligned} Y &= L\cos\psi\frac{n\sigma}{n'\sigma'}, \\ Z &= L\sin\psi\frac{n\sigma}{n'\sigma'}. \end{aligned} \tag{48}$$

The formula (47) proves, that the longitudinal aberrations are proportional to the magnitude of the vector $\boldsymbol{L}$ and do not depend upon the magnitude of $\boldsymbol{M}$. Therefrom it may be inferred that the astigmatic images of the line passing through the coordinate origin have the shape of two lines of equations

$$\frac{X}{\varepsilon[K_{\mathrm{IV}}\cos(\psi-\vartheta_4)\pm K_{\mathrm{III}}]} = \frac{Y}{\cos\psi} = \frac{Z}{\sin\psi}, \tag{49}$$

where

$$\varepsilon = (p-s)\frac{n'}{n}.$$

The Equation (49) results after the elimination of $\boldsymbol{L}$ from (47) and (48). The angle between these lines is a.

The application of the known formula of the analytical geometry for the sine of the angle between two lines gives

$$\sin a = 2\varepsilon K_{\mathrm{III}}. \tag{50}$$

By elimination of the parameter ψ from Eq. (49) we obtain the equation of a quadric surface, which is the astigmatic image of the plane perpendicular to the axis of reference

$$(X-\varepsilon K_{\mathrm{IV}}\cos\vartheta_4\, Y-\varepsilon K_{\mathrm{IV}}\sin\vartheta_4 Z)^2 = (Y^2+Z^2)K_{\mathrm{III}}^2\varepsilon^2. \tag{51}$$

If $\boldsymbol{K}_{\mathrm{III}} \neq 0$ it is a circular cone.

The plane

$$X-\varepsilon K_{\mathrm{IV}}\cos\vartheta_4\, Y-\varepsilon K_{\mathrm{IV}}\sin\vartheta_4 Z = 0 \tag{52}$$

is the symmetry plane of the conic surface (51). The normal to the plane (52), passing through the origin, of equation

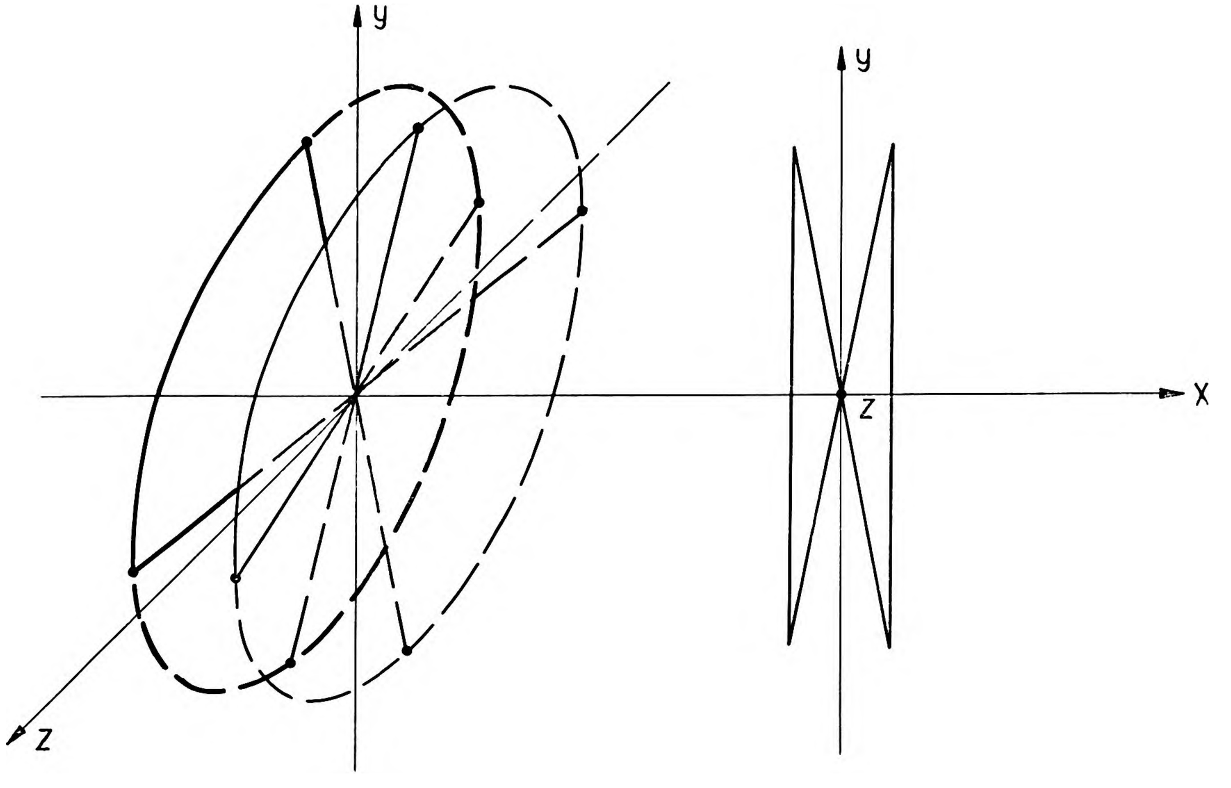

Fig. 7. The surface of the astigmatic image in the shape of a cone symmetrical with respect to coordinate axis, if $\boldsymbol{K}_{\mathrm{IV}} = 0$

$$X = -\frac{Y}{\varepsilon K_{IV}\cos\vartheta_4} = -\frac{Z}{\varepsilon K_{IV}\sin\vartheta_4} \tag{53}$$

is the axis of the cone. The axis of cone makes an angle β, with the axis of reference or the x-axis, approximately

$$\sin\beta = \varepsilon K_{IV}. \tag{54}$$

The lines (49) are, at the same time, the generatrices of the cone and make an angle γ with the axis of the cone and

$$\cos\gamma = \pm\varepsilon K_{III} \tag{55}$$

is a half angle of the cone.

The formulas (49) to (55) prove, that the astigmatic images of lines passing through the coordinate origin form two lines, with a small angle a, depending on the vector $\boldsymbol{K}_{III}$ between them. The astigmatic images of a plane arise on a conic surface and the measure of the inclination of the cone axis is the vector $\boldsymbol{K}_{IV}$, while the measure of the half angle is the vector $\boldsymbol{K}_{III}$. The vector $\boldsymbol{K}_{IV}$ determines the inclination of the image and vector $\boldsymbol{K}_{III}$ its astigmatism. If $\boldsymbol{K}_{III} = 0$, then the image of any line is one straight line, and the image of the plane is one inclined plane represented by the Eq. (52). It can be shown that if $\boldsymbol{K}_{III} \neq 0$, the image of a line not passing through the origin is a hyperbole, both the branches of which corresponding to both the astigmatic images.

The Figure 7, which similarly as Fig. 3 illustrates the case $\boldsymbol{K}_{IV} = 0$, represents a cone symmetrical to the coordinate system with the x-axis as the cone axis. Figure 8 corresponding to Fig. 4 ($\boldsymbol{K}_{III} = 0$) demonstrates an inclined plane. Figure 9 exhibits a cone with the axis inclined towards the x-axis, because $\boldsymbol{K}_{III}$ and $\boldsymbol{K}_{IV}$ differ from zero. It corresponds with the transverse aberrations shown in the Fig. 5 and 6.

The formula (55) proves, that the cos γ is a small quantity, hence the angle γ differs a little from a right angle.

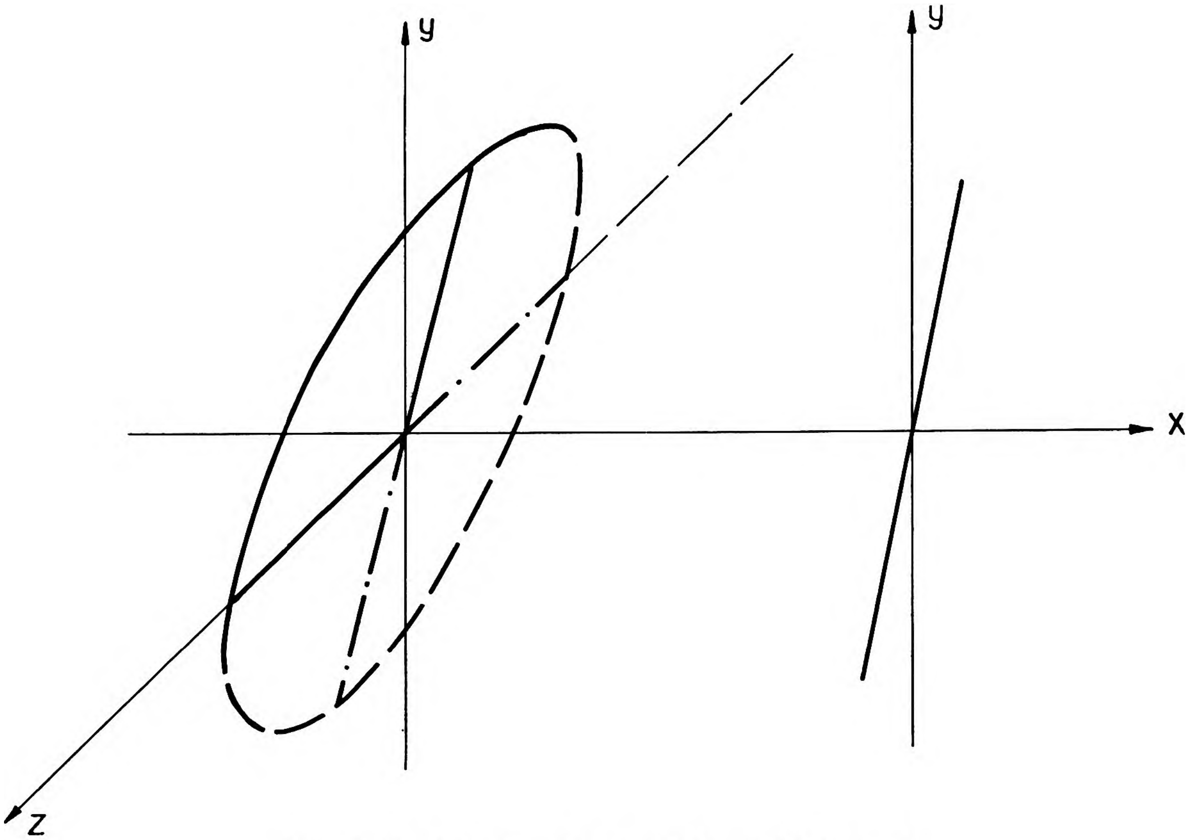

Fig. 8. The inclined surface of the image, if $\boldsymbol{K}_{III} = 0$

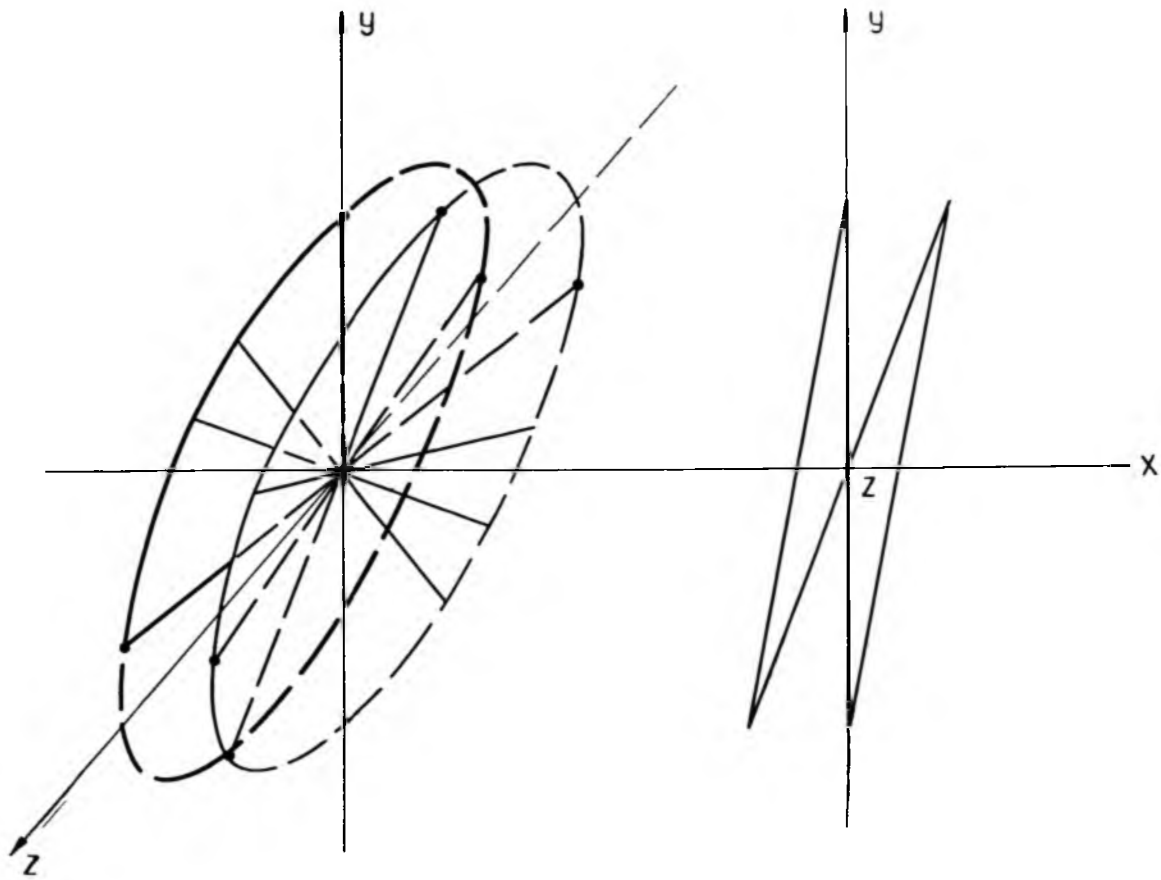

Fig. 9. The surface of the image as an inclined cone

Distortion

The distortion of decentration depends upon the square of the field magnitude. For each decentration the two independent aberration coefficients C_{V} and C_{VI} appear. Two resultant vectors are defined as the linear superposition of the products of the decentration vectors of several surfaces by their aberration coefficients according to the formulas

$$\boldsymbol{K}_{\mathrm{V}} = \frac{n^2\sigma^2}{n'\sigma' J^2} \Sigma \boldsymbol{c}_k \varrho_k C_{\mathrm{V},k}, \tag{56}$$

$$\boldsymbol{K}_{\mathrm{VI}} = \boldsymbol{K}_{\mathrm{V}} + \frac{n^2\sigma^2}{n'\sigma'} \Sigma \boldsymbol{c}_k \varrho_k C_{\mathrm{VI},k}. \tag{57}$$

The angles of the vectors $\boldsymbol{K}_{\mathrm{V}}$ and $\boldsymbol{K}_{\mathrm{VI}}$ with the y-axis are denoted by ϑ_5 and ϑ_6. Let the vector $\boldsymbol{L}$ determine the position of any point on the object plane. The image coordinates Y and Z of this point, with regard to (21), (31), (56) and (57), are

$$\begin{aligned} Y &= GL_y + \frac{L^2}{2} K_{\mathrm{VI},y} + L_y L_z K_{\mathrm{V},z} + L_y^2 K_{\mathrm{V},y}, \\ Z &= GL_z + \frac{L^2}{2} K_{\mathrm{VI},z} + L_z^2 K_{\mathrm{V},z} + L_y L_z K_{\mathrm{V},y}. \end{aligned} \tag{58}$$

$$G = \frac{n\sigma}{n'\sigma'}$$

denotes the transversal magnification.

Let a straight line be located in the object plane at a distance A from the coordinate origin making an angle u with respect to the y-axis (Fig. 10).

The parameter T denotes the distance of the considered point on the line from the point nearest to the coordinate origin (Fig. 10).

$$\begin{aligned} L_y &= -A\sin u + T\cos u, \\ L_z &= A\cos u + T\sin u. \end{aligned} \tag{59}$$

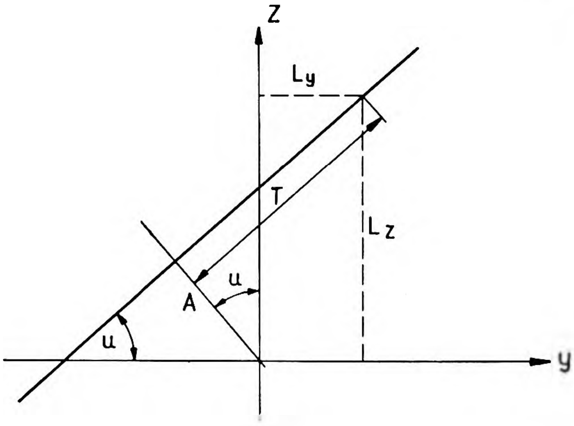

Fig. 10. A straight line in parametric form, where A is its distance from the coordinate origin, u its angle with y-axis, T current parameter equal to the distance of the current point on the line to the point nearest to the coordinate origin

The image of the straight line is a conic

$$\begin{aligned} Y &= -AG\sin u + A^2\left[\frac{K_{\mathrm{VI}}\cos\vartheta_6}{2} + K_{\mathrm{V}}\sin u\sin(u-\vartheta_5)\right] + T[G\cos u + AK_{\mathrm{V}}\sin(\vartheta_5 - 2u)] + \\ &\quad + T^2\left[\frac{K_{\mathrm{VI}}}{2}\cos\vartheta_6 + K_{\mathrm{V}}\cos u\cos(u-\vartheta_5)\right], \\ Z &= AG\cos u + A^2\left[\frac{K_{\mathrm{VI}}}{2}\sin\vartheta_6 + K_{\mathrm{V}}\cos u\sin(\vartheta_5 - u)\right] + T[G\sin u + AK_{\mathrm{V}}\cos(\vartheta_5 - 2u)] + \\ &\quad + T^2\left[\frac{K_{\mathrm{VI}}}{2}\sin\vartheta_6 + K_{\mathrm{V}}\sin u\cos(u-\vartheta_5)\right]. \end{aligned} \tag{60}$$

The Equations (60) have been obtained combining L_y, L_z from (59) with the Equations (58). The current parameter of the curve is the magnitude T. The curvature of the curve, as determined by (60) is easy to calculate with the help of the known formula

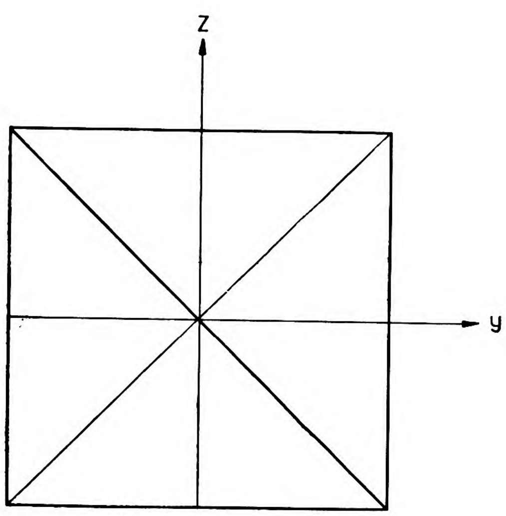

Fig. 11. The object as a square with the symmetry axis

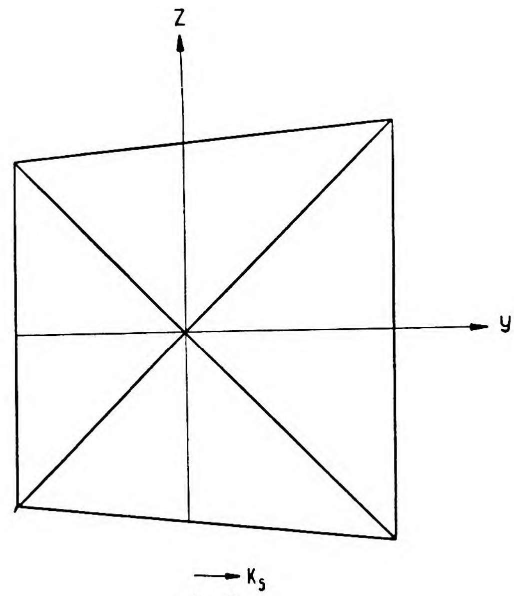

Fig. 12. The image of a square is a trapezium, if $K_{\mathrm{VI}} = 0$

$$\varrho = \frac{Y'_T Z''_T - Y''_T Z'_T}{(Y'^2_T + Z'^2_T)^{3/2}}.$$

The omission of the squares and products with respect to $\boldsymbol{K}_{\mathrm{V}}$ and $\boldsymbol{K}_{\mathrm{VI}}$ reduces it to the following

$$\varrho = \frac{K_{\mathrm{V}} \sin(u - \vartheta_6)}{G^2}. \tag{61}$$

The formula (61) proves that, providing $\boldsymbol{K}_{\mathrm{VI}} = 0$ the image of the straight line is a straight line. If $\boldsymbol{K}_{\mathrm{VI}} \neq 0$ the images of lines parallel to the vector $\boldsymbol{K}_{\mathrm{VI}}$ are lines.

The equation of the tangent to the curve (60) may be written on the base of the known formula

$$\frac{Y-y}{Y'_T} = \frac{Z-z}{Z'_T}. \tag{62}$$

From Equation (60) it follows that

$$\begin{aligned} Y'_T &= \cos u + \frac{AK_{\mathrm{V}}}{G} \sin(\vartheta_5 - 2u) + \frac{T}{G}[K_{\mathrm{VI}} \cos\vartheta_6 + 2K_{\mathrm{V}} \cos u \cos(\vartheta_5 - u)], \\ Z'_T &= \sin u + \frac{AK_{\mathrm{V}}}{G} \cos(\vartheta_5 - 2u) + \frac{T}{G}[K_{\mathrm{VI}} \sin\vartheta_6 + 2K_{\mathrm{V}} \sin u \cos(u - \vartheta_5)]. \end{aligned} \tag{63}$$

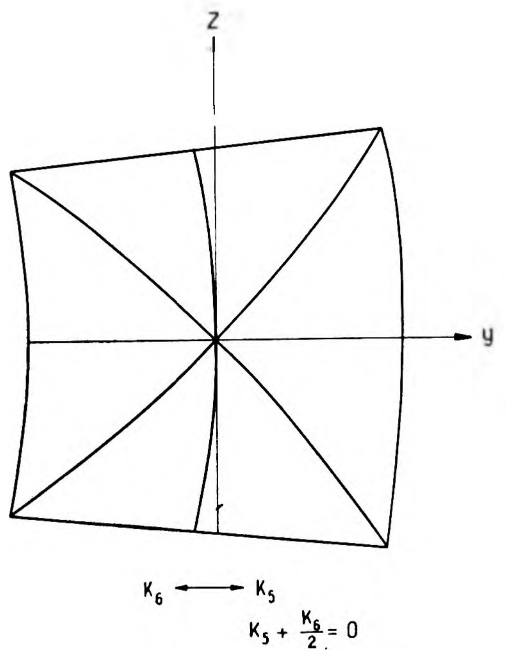

Fig. 13. The image of a square, if the vectors $\boldsymbol{K}_{\mathrm{V}}$ and $\boldsymbol{K}_{\mathrm{VI}}$ have the same directions themselves as the y-axis

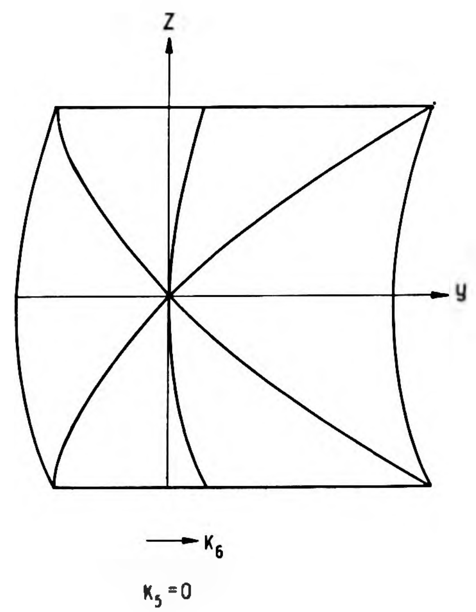

Fig. 14. The image of a square, if $\boldsymbol{K}_{\mathrm{V}} = 0$. The images of the sides parallel to the vector $\boldsymbol{K}_{\mathrm{VI}}$ form the parallel lines and those of the sides perpendicular to $\boldsymbol{K}_{\mathrm{VI}}$, form two parallel parabolas

For the angle δ between the tangent described by the formulas (62) and (63), and the line of the Gaussian image we have

$$\sin\delta = \frac{AK_{\mathrm{V}}}{G} \cos(u - \vartheta_5) + \frac{TK_{\mathrm{VI}}}{G} [\sin(\vartheta_6 - u)]. \tag{64}$$

The formula (64) shows, that for $\boldsymbol{K}_{\mathrm{V}} = 0$, the tangents to the curve (60) at the point nearest to the coordinate origin are not inclined. Also the images of lines perpendicular to $\boldsymbol{K}_{\mathrm{V}}$ are not inclined. The tangents to the curve (60) at the origin of coordinate system ($T = 0$, $A = 0$) are not inclined, too. The vector $\boldsymbol{K}_{\mathrm{VI}}$ causes a "curvature" of the line image and $\boldsymbol{K}_{\mathrm{V}}$ the "inclination" of the image.

The Figure 11 represents a square with its diagonales and symmetry axes. The Figures 12 to 15 present the images of this figure in some different special cases. The images for the case $\boldsymbol{K}_{\mathrm{VI}} = 0$ are illustrated in the Figure 12. The image of a square is a trapezium. The images of the straight lines perpendicular to the vector $\boldsymbol{K}_{\mathrm{V}}$ are parallel straight lines. The Figure 13 shows the image in the case $\boldsymbol{K}_{\mathrm{VI}} = -2\boldsymbol{K}_{\mathrm{V}}$.

The Figure 14 illustrates the case $\boldsymbol{K}_{\mathrm{V}} = 0$. A set of lines parallel to $\boldsymbol{K}_{\mathrm{VI}}$ produce a set of parallel lines as the image. If a set of parallel lines is not parallel to vector $\boldsymbol{K}_{\mathrm{VI}}$, then their images form a family of parallel parabolas.

The axis of symmetry of the Figures 12, 13 and 14 is the y-axis which is the direction of the vectors $\boldsymbol{K}_{\mathrm{V}}$ and $\boldsymbol{K}_{\mathrm{VI}}$. On the Figure 15 both the vectors differ from zero and do not exhibit any symmetry.

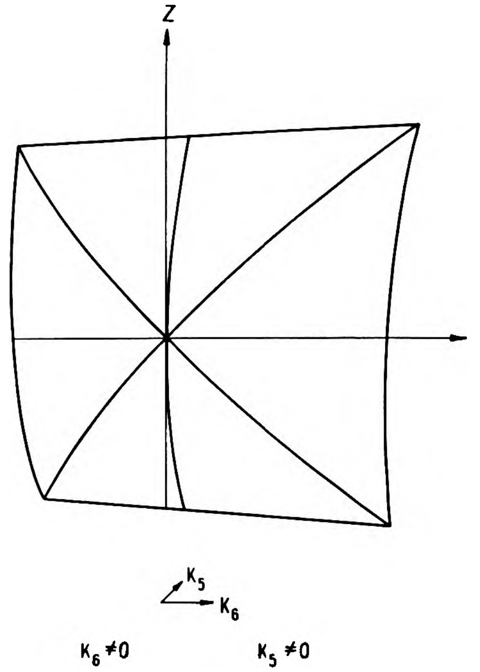

Fig. 15. The general case of the image of a square

Decentred plane

The foregoing formulas relate to a system of decentred spherical surfaces. Their modification for plane surfaces is not difficult.

The Figure 16 represents the normal N_0 to decentred surface in its vertex. On the base of this figure and of the formula (11) or (16) we may write for the cosines of this normal

$$N_{0,x} = 1,$$

$$N_{0,y} = \varrho c_y,$$

$$N_{0,z} = \varrho c_z.$$

The angle between this normal and the axis of reference is

$$\eta \approx \sin\eta = \varrho c.$$

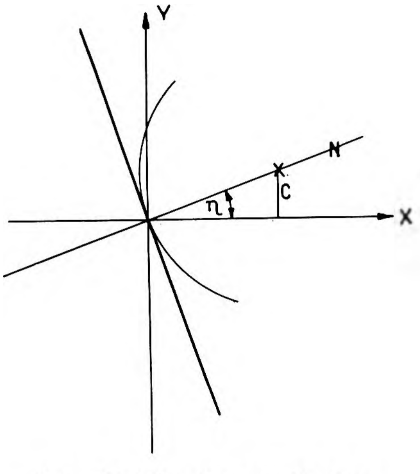

Fig. 16. The decentred plane

As it is shown on the Fig. 16, if $\varrho \to 0$ then $c \to \infty$, but the product $\eta = \varrho c$ remains finite and is the measure of the decentricity for the spherical and plane surfaces. Substituting in all the equations the product ϱc by the magnitude of the angle η we obtain the formulas valid for the decentred planes.

Object at infinity

In the foregoing considerations it was assumed, that the object and the entrance pupil were, at a finite distance. The formulas deduced above can be easily transformed to remain valid for the object infinitely removed, as will be shown on some examples. We have only to replace the object coordinates by the coordinates of its perfect image according to the formulas

$$L = L_0' \frac{n'\sigma'}{n\sigma}; \quad G = \frac{n\sigma}{n'\sigma'},$$

$$J = n\sigma\omega(p-s) = n'\sigma'\omega'(p'-s').$$

In the formula (37) we have to introduce only slightly different factors

$$K_{\mathrm{III}}' = \frac{1}{G} K_{\mathrm{III}} = \frac{\omega n}{J^2 n'} \Sigma c_k \varrho_k C_{\mathrm{III},k},$$

$$K_{\mathrm{IV}}' = \frac{1}{G} K_{\mathrm{IV}}.$$

The semi-axes of the ellipse are now (41)

$$\varrho_{1,2} = [K_{\mathrm{IV}}' \cos(\psi - \vartheta_4) \pm K_{\mathrm{III}}'] M L_0'.$$

The formulas (50) to (55) will remain valid for the object at infinity, if we substitute K_{III}' and K_{IV}' for K_{III} and K_{IV} and

$$\varepsilon' = \frac{J}{n\omega\sigma'}$$

for ε.

Instead of the vectors K_{V} and K_{VI} we have to introduce the vectors K_{V}' and K_{VI}', defined as

$$K_{\mathrm{V}}' = \frac{1}{G^2} K_{\mathrm{V}}^2,$$

$$K_{\mathrm{VI}}' = \frac{1}{G^2} K_{\mathrm{VI}}.$$

Instead of the straight line in the object plane (59) we examine a straight line in the plane of the perfect image

$$L_{0,v}' = -A' \sin u + T' \cos u.$$

With respect to the small changes the formulas (56) to (64) remain valid for the object at infinity. Formula (64) becomes

$$\sin\delta = A' K_{\mathrm{V}}' \cos(u - \vartheta_5) + T' K_{\mathrm{VI}}' \sin(\vartheta_6 - u).$$

In a similar manner all the relations can be transformed so as to remain valid for the case of the entrance pupil lying at infinity. However, that case will not be considered in detail.

Conclusions

The aberrations of decentred systems have been examined under the assumption, that the decentrations are not great and reduced to the displacement of the centers of curvature of the refracting surfaces in the direction perpendicular to the axis of reference. In reality, the optical systems are built up from lenses, which undergo pure decentration and tilts. In this second case the displacements of the surface will not be exactly perpendicular to the axis of reference. It is easy to show, that the longitudinal components of the displacement are not great and are proportional to the square of the magnitude of vector c, which have been omitted in our considerations.

The comparison of the numerical results of the ray tracing with the second order aberrations shows an astonishing agreement of results even for the systems with large apertures.

Об аберрациях незначительно нецентрических систем в области Зейдела

Описывается аберрация „второго" ряда в области Зейдела слегка нецентрической системы, лишённой симметрии, состоящей из нецентрических сферических и плоских поверхностей. Определяется шесть векторных аберрационных коэффициентов. Векторы эти образуются линейной суперпозицией векторов нецентричности скалярными аберрационными коэффициентами. Легко можно вычислить скалярные аберрационные коэффициенты отдельных поверхностей, если известны аберрации 3-го ряда аналогичной центрической системы. Вектор K_{I} определяет „биение" изображения. Вектор K_{II} описывает кому, пропорциональную квадрату апертуры. Аберрации, пропорциональные произведению величины апертуры и поля, определяют два вектора. Вектор K_{III} можно назвать вектором астигматизма или „конусности" поверхности. Вектор K_{IV} определяет наклон плоскости изображення. Дисторсия завнсит от двух векторов. Вектор K_{VI} определяет искривление, а вектор K_{V} — непараллельность изображения прямых.

References

[1] Bartkowska, J., *On the Inclination of the Image Plane in an Optical System caused by Slightly Decentred Surfaces*, Acta Phys. Pol., XXV, 4 (1964), ss. 551–563.

[2] Bartkowska, J., *Principal Points, Cardinal Axis and Focal Planes of Slightly Decentred Optical System*, Acta Phys. Pol., XXVI (1964), ss. 1101–1113.

[3] Cox, A., *A System of Optical Design*, Focal Press, London–New York 1964.

[4] Hofmann, Ch., *Definition und Messung der Dezentrierung sphärischer Einzellinsen*, Exp. Techn. Phys., 9 (1961), s. 145.

[5] Maréchal, A., *Etude des Aberrations d'Excentrement Tolerances sur le Centrage des Instruments*, d'Optique, 29, 1 (1950), ss. 1–24.